PROCEEDINGS OF SCIENCE

Pole trajectories of the $\Lambda(1405)$ towards the SU(3) limit

Raquel Molina,[a,*] **Zejian Zhuang,**[a] **Jun-Xu Lu**[b] **and Li-Sheng Geng**[b,c,d,e]

[a] *Departamento de Física Teórica and IFIC, Centro Mixto Universidad de Valencia-CSIC Institutos de Investigación de Paterna, Aptdo.22085, 46071 Valencia, Spain*

[b] *School of Physics, Beihang University, Beijing 102206, China*

[c] *Beijing Key Laboratory of Advanced Nuclear Materials and Physics, Beihang University, Beijing 102206, China*

[d] *Peng Huanwu Collaborative Center for Research and Education, Beihang University, Beijing 100191, China*

[e] *Southern Center for Nuclear-Science Theory (SCNT), Institute of Modern Physics, Chinese Academy of Sciences, Huizhou 516000, China*

E-mail: rmolina@ific.uv.es

We determine for the first time the quark mass dependence of the $\Lambda(1405)$ from an analysis of a recent LQCD simulation on the $\pi\Sigma - \bar{K}N$ scattering in $I = 0$ and the trajectories of these poles towards the symmetric point over the $m_u + m_d + m_s$ = constant trajectory accurately. At $m_\pi \simeq 200$ MeV, our results are consistent with both, the lattice simulation and experimental data. We predict qualitatively similar trajectories at LO and up to NLO, consistent with the LO interaction's dominance. At the SU(3) symmetric point of this trajectory, both poles are on the physical sheet, and the lower pole is located at $E^{(1)} = 1573(6)(6)$ MeV, becoming a SU(3) singlet, while the higher pole at $E^{(8a)} = 1589(7)(5)$ MeV couples to the octet representation. The results presented here are crucial to shed light on the molecular nature of this exotic baryon and can be tested in future LQCD simulations.

QCHSC24
19-24 August, 2024
Cairns Convention Centre, Cairns, Queensland, Australia

*Speaker

PoS(QCHSC24)096

1. Introduction

Being one of the first exotic baryon resonances discovered, the $\Lambda(1405)$ [1, 2] has been a subject of controversy for a long time. The reason is the two-pole structure predicted in the chiral unitary approach, closely related to $\pi\Sigma$ and $\bar{K}N$ thresholds [3–9]. Sixty years after its discovery, the lower pole has been included in the PDG [10]. In addition, it is the first negative parity excitation of the Λ state, however, it is lighter than its nucleon counterpart by around 100 MeV. These features can be reproduced in the chiral unitary approach [3, 5]. In the chiral-unitary formalism, the main interaction is driven by the lowest order (LO) interaction in s-wave, the so-called Weinberg-Tomozawa term, which is attractive and leads to two poles in the unphysical sheet, also present at NLO and NNLO [11–15]. In this approach, the lower-energy pole couples more strongly to $\pi\Sigma$ and the higher one to $\bar{K}N$. The analysis of experimental cross sections with Hamiltonian effective field theory leads also to the two-pole structure [16]. For recent reviews of the $\Lambda(1405)$, see Refs. [8, 9].

Lattice QCD (LQCD) simulations related to the $\Lambda(1405)$ were conducted in the past considering only single-baryon three-quark interpolating fields [17–19]. The chiral unitary approach predicts different trends of the two poles of the $\Lambda(1405)$ towards the SU(3) limit. In this limit, while the low-energy pole belongs to the singlet representation, the higher one does to the octet [5, 20]. First explorations of the trajectories of the $\Lambda(1405)$ with increasing pion masses can be found in Refs. [21–25]. Recently, a LQCD simulation included the meson-baryon operators and a signature of the lower pole of the $\Lambda(1405)$ has been observed in LQCD for the first time [26, 27]. In this work, we predict the trends of these poles towards the SU(3) limit from this data within the NLO chiral unitary approach. The data of [26, 27] are based on the light hadron ensembles of [28] in a chiral path of the type $\mathrm{Tr}[M] = C$.[1] These trajectories are connected to the SU(3) breaking pattern and the dynamically-generated-resonance nature of the $\Lambda(1405)$.

2. Formalism

The details of the calculation are presented in [29]. We study the sector *isospin, strangeness*, $I = 0, S = -1$, considering four channels $i, j = \pi\Sigma, \bar{K}N, \eta\Lambda, K\Xi$, and including the LO (also with Born diagrams) and NLO terms,

$$V_{ij} = V_{ij}^{\mathrm{LO}} + V_{ij}^{\mathrm{NLO}}, \tag{1}$$

where $V^{\mathrm{LO}} = V^{\mathrm{WT}} + V^{\mathrm{Born}}$. These are given by [30],

$$V_{ij}^{\mathrm{WT}} = -\frac{N_i N_j}{4f^2}\left[C_{ij}\left(2\sqrt{s} - M_i - M_j\right)\right], \quad V_{ij}^{\mathrm{NLO}} = -\frac{N_i N_j}{f^2}\left(D_{ij} - 2k_\mu k'^\mu L_{ij}\right), \tag{2}$$

where $N_i = \sqrt{(M_i + E_i)/2M_i}$, and M_i, E_i stand for the baryon mass and energy of channel i, respectively. Apart from the Weinberg-Tomozawa (WT) and the NLO interaction, the Born terms for the s- and u-channels with the $J^P = 1/2^+$ octet baryon-exchange diagrams are included, which are taken from Ref. [31]. The D_{ij} and L_{ij} coefficients are a combination of the pertinent LECs of b_0, b_D, b_F, and d_i, $i = 1, 4$. The LECs b_i are fitted to the recent RQCD simulations on the quark mass dependence of baryon masses for the CLS ensembles [28], which include data on

[1] Here, M stands for the quark mass matrix, and the trajectory $\mathrm{Tr}[M] = C$ means $m_u + m_d + m_s = C$.

the $m_s = m_{s,\text{phy}}$, $\text{Tr}[M] = C$ and $m_{u(d)} = m_s$ trajectories. The result of this fit can be seen in [29]. For the $\text{Tr}[M] = C$ path, the SU(3) limit is reached at $m_\pi = 423$ MeV with a baryon mass $m_B = 1182(7)(5)$ MeV. We take the quark mass dependence of the pseudoscalar meson masses m_ϕ and decay constants f_ϕ, with $\phi = \pi, K, \eta$, from the global fit performed in [32].

In the finite volume, neglecting the effects from higher partial waves, the scattering amplitude reads,

$$\tilde{T}^{-1} = V_0^{-1} - \tilde{G} \, . \tag{3}$$

where V_0 stands for the s-wave NLO interaction. The finite-volume loop function $\tilde{G}$ can be calculated in the DR scheme as,

$$\widetilde{G}(P) = G^{\text{DR}}(P) + \lim_{q'_{\text{max}} \to \infty} \Delta G(P, q'_{\text{max}}), \tag{4}$$

being $\Delta G = \tilde{G}^{\text{co}} - G^{\text{co}}$, the loop function in the infinite volume, G^{DR} or G^{co}, and the one in the finite volume, $\tilde{G}^{\text{co}}$ [21, 29]. In the infinite volume, we use G^{DR} with a quark-mass-dependent subtraction constant [29, 33], $\alpha(q_{\text{max}})$. Neglecting the effects from higher partial waves, the energy levels are given solely by [29],

$$\det\left[I - V_0 \tilde{G}\right] = 0. \tag{5}$$

3. Results and discussions

We analyze the energy levels of Refs. [26, 27] for $m_\pi \simeq 200$ MeV through Eq. (5), with the s-wave projection of the NLO interaction in Eq. (1). The resulting energy levels are shown in Fig. 1. The LQCD energy levels are very well reproduced by the interaction up to NLO. We have included the first four energy levels in the fit, with all data points shown in Fig. 1. The d_i LECs are fitted to the energy levels. The value of the reduced-χ^2 obtained is $\chi^2_{\text{dof}} = 2.3$. [2] The cutoff q_{max} obtained in this fit is 623(23)(23) MeV.

d_1	d_2	d_3	d_4
−0.38(9)(7)	0.02(1)(1)	−0.07(3)(3)	−0.45(5)(6)

Table 1: Results for the LECs d_i in units of GeV^{-1}. The second error comes from the uncertainty in the lattice spacing [26, 27].

In the infinite volume limit, we find two poles related to the $\Lambda(1405)$, one is a virtual pole and the other a resonance. In Table 2, we give the positions and couplings of the poles to the different channels for $m_\pi = 138$ and 200 MeV, for the four-coupled-channel calculation in the first and second rows, respectively. When the $\eta\Lambda$ and $K\Xi$ channels are removed, the virtual resonance related to the lower pole becomes a virtual bound state. The pole positions and couplings for the two-coupled channel system are shown in the third row, which can be compared with the LQCD simulation results [26, 27]. The positions of the two poles at $m_\pi \simeq 200$ MeV and the ratios of the couplings obtained in this work for two channels have an excellent agreement with the ones from

[2] We do not consider systematic errors in the LQCD data when performing the fit.

LQCD [26, 27]. While the first pole couples strongly to $\pi\Sigma$, the second one does to $\bar{K}N$. In the four-coupled-channel calculation, the couplings to the $\eta\Lambda$ and $K\Xi$ are non-negligible. Note that these channels were not considered in the analysis of the LQCD simulation [26, 27].

The positions of the poles at the physical point agree also well with experiment [29] and also the experimental cross sections are fairly reproduced from the LQCD analysis. See Fig. 2. This strongly supports the quark-mass dependence obtained here.

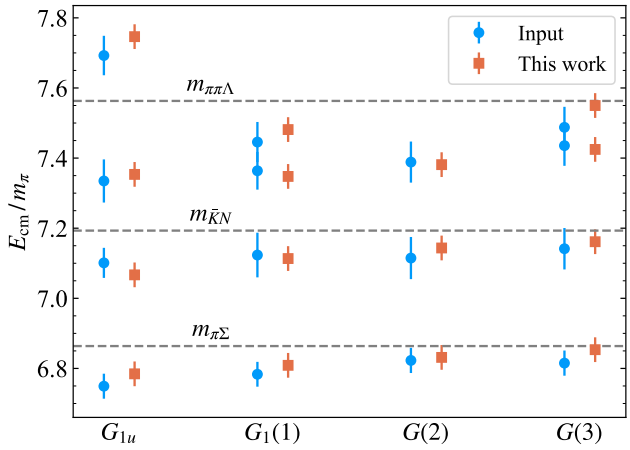

Figure 1: Finite-volume spectrum [26, 27] in the center-of-mass frame used as inputs to constrain the LECs of the chiral Lagrangian up to NLO.

Next, we comment on the results obtained in the SU(3) limit. In this limit, we obtain a resonance coupling to the singlet representation corresponding to the lower pole and two poles coupling to the octet representations. Note that, in principle, the pseudoscalar meson-baryon channels couple to both, 8 and 8′ representations[3], and therefore, the resonance generated by them can also couple to both, mixing these representations [20]. Since the SU(3) symmetry is respected in this limit, it is possible to find a basis where the octet representations disentangle by diagonalizing the interaction [29] and to find the mixing angle we follow [20]. We have obtained $\theta \simeq -60°$. The pole positions and couplings to the different representations are shown in Table 3. With only WT, we find one pole located at $E^{(1)} = 1556(2)$ and two degenerate poles at $E^{(8a)} = E^{(8b)} = 1606(1)$ MeV, coupling to the singlet and octet representations, respectively. Note that this degeneracy is *accidental* caused by the WT interaction. When the Born and NLO terms are included, the two higher poles split in energy. This effect is in agreement with findings from previous works [5, 20, 23]. In particular, while the lower pole couples to the $8a$, the higher one does to the $8b$ representation. The mass shift between the two higher poles after including the NLO obtained in this work is $\Delta E^{(8)} = 14$ MeV.

Next, we show our prediction for the trajectories of the poles towards the SU(3) limit over the $\mathrm{Tr}[M] = C$ trajectory in Fig. 3 (a), where we show the results at LO and up to NLO. We see that, at LO (LO+NLO), the lower pole evolves from a resonance into a virtual state at $m_\pi = 198$ (174) MeV. Then, it becomes a bound state at $m_\pi = 235$ (273) MeV and a singlet pole when it reaches the symmetric line. On the other hand, the higher pole changes from a resonance to a bound state

[3] In particular, the $\bar{K}N$ channel couples to both octet representations, 8 and 8′.

at $m_\pi = 415$ (405) MeV, close to the symmetric point. The higher pole of the $\Lambda(1405)$ and the $\Lambda(1670)$ couple to the $8a$ and $8b$ representations in the SU(3) limit.

# ch	m_π	Pole	$\lvert g_{\pi\Sigma}\rvert$	$\lvert g_{\bar{K}N}\rvert$	$\left\lvert \frac{g_{\pi\Sigma}}{g_{\bar{K}N}} \right\rvert$	$\lvert g_{\eta\Lambda}\rvert$	$\lvert g_{K\Xi}\rvert$
4	138	$1376(10)(10) - i142(19)(5)$	2.8(1)(2)	2.3(6)(3)	1.2(5)(1)	1.5(3)(3)	1.0(1)(2)
		$1418(11)(2) - i11(6)(3)$	1.1(5)(2)	3.0(2)(2)	0.4(1)(1)	2.0(2)(5)	0.4(1)(3)
	200	$1366^{(43)(19)}_{(6)(3)} - i57^{(42)(23)}_{(57)(57)}$	3.7(7)(4)	1.8(8)(6)	2.1(5)(3)	1.2(3)(3)	0.8(2)(2)
		$1450(15)(11) - i15(9)(5)$	1.5(7)(4)	3.1(5)(4)	0.5(2)(1)	2.1(3)(6)	0.5(1)(3)
2	200	1387(7)(6)	3.4(10)(10)	1.8(5)(8)	1.9(10)(5)	...	...
		$1455(14)(6) - i29(11)(7)$	2.2(7)(3)	3.8(6)(3)	0.6(1)(1)	...	...

Table 2: Pole positions and couplings of the $\Lambda(1405)$ for $m_\pi = 138$ and 200 MeV. m_π and the pole position are given in units of MeV.

	WT			LO [WT+Born]			LO+NLO		
	z_1	z_2	z_3	z_1	z_2	z_3	z_1	z_2	z_3
Pole	1556(2)	1606(1)	1606(1)	1548(3)	1601(1)	1607(1)	1573(6)(6)	1589(7)(5)	1603(9)(10)
$\lvert g_{(1)}\rvert$	3.0(1)	0	0	3.0(1)	0	0	2.8(1)(1)	0	0
$\lvert g_{(8_a)}\rvert$	0	0.8(1)	0	0	1.8(1)	0	0	2.4(8)(2)	0
$\lvert g_{(8_b)}\rvert$	0	0	0.8(1)	0	0	0.4(1)	0	0	1.7(6)(5)

Table 3: Pole positions and couplings to the relevant multiplets in the SU(3) limit. The pole position is given in units of MeV.

The prediction for the evolution of the two poles over the $m_s = m_{s,\text{phy}}$ trajectory is shown in Fig. 3 (b). In this case, we obtain that the symmetric point corresponds to $m_\pi = 758$ MeV. However, at this high pion mass, the NLO ChPT expansion breaks down [29], and in particular, the expressions of the decay constants f_ϕ, $\phi = \pi, K, \eta$ fail. Still, we can make predictions up to 450 MeV, were the NLO ChPT relations for the masses and pseudoscalar decay constants work well [32]. These values are also consistent with previous analysis of the baryon masses [34]. Since now the $\bar{K}$ and the Σ masses increase with the pion mass [29], we obtain that the real parts of the two poles, which couple significantly to $\bar{K}N$ and $\pi\Sigma$, rise much faster than in the $\text{Tr}[M] = C$ trajectory. In the $m_s = m_{s,\text{phy}}$ trajectory, the lower pole evolves from a resonance into a virtual state at $m_\pi = 200$ (178) MeV at LO (LO+NLO). Then, it becomes a bound state at $m_\pi = 236$ (278) MeV. The poles corresponding to the $\Lambda(1405)$ and $\Lambda(1670)$ are always found in the second Riemann sheet as resonances below $m_\pi = 450$ MeV. These results can be tested in future LQCD simulations.

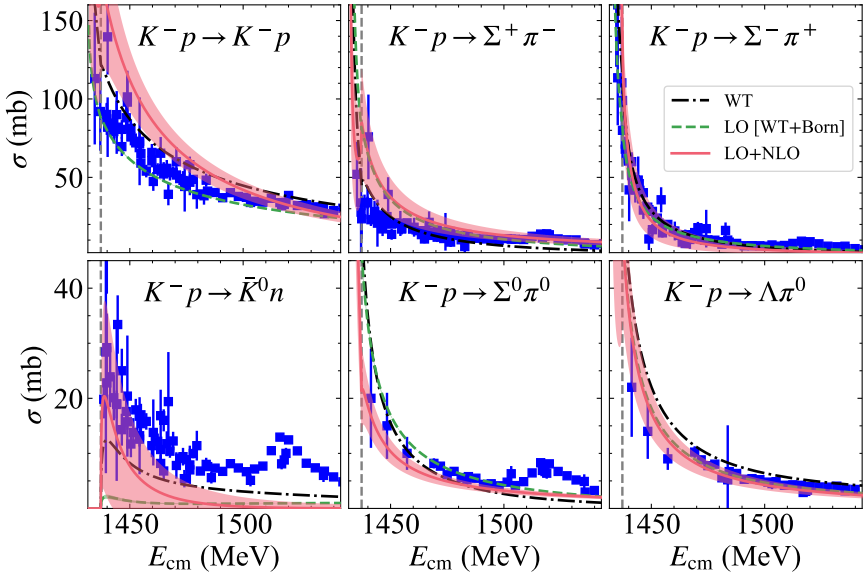

Figure 2: Comparison of the predicted cross-sections and the experimental data [8]. The error bands of the cross sections are constrained by the correlation matrix of the fit to the LQCD energy levels.

4. Conclusion and outlook

In this work, we have analyzed LQCD data on $\pi\Sigma - \bar{K}N$ scattering for $I = 0$ (energy levels) at $m_\pi \simeq 200$ MeV and LQCD octect-baryon masses data in the range of pion masses between the physical point and $m_\pi = 450$ MeV. The theoretical framework is based on the NLO chiral Lagrangians for the meson-baryon interaction and covariant baryon chiral perturbation theory for the baryon masses. Our analysis took into account recent LQCD data on the baryon masses, meson masses, and pseudoscalar decay constants, and the subtraction constants turn out to be of natural size in the range of pion masses considered. Therefore, we have obtained the most precise determination of the trajectories of the two-pole $\Lambda(1405)$ toward the symmetric line on the $\mathrm{Tr}[M] = C$ curve. The extrapolation of our results to the physical point is consistent with the experiment. Remarkably, our results also agree with the cross-section data. Thus, consistency between the chiral unitary approach predictions for the two-pole structure, the recent LQCD scattering data [26, 27], and the experimental data, is shown for the first time. We found that both poles lie on the physical Riemann sheet at the symmetric point at $m_\pi = 423$ MeV. Concretely, at the SU(3) limit, we find one of the $\Lambda(1405)$ poles couples to the singlet and is located at $E^{(1)} = 1573(6)(6)$ MeV, while the higher one appears at $E^{(8a)} = 1589(7)(5)$ MeV and couples to the octet representation. There is a third pole found connected to the $\Lambda(1670)$, shifted by 14 MeV and belonging to the $8b$ representation. The results obtained here strongly support the two-pole structure of the $\Lambda(1405)$ generated from the $\pi\Sigma - \bar{K}N$ interaction. We have shown that the additional LQCD data also supports the two-pole structure consistently with the experiment. The present work can also be tested in future LQCD simulations and experimental measurements [35].

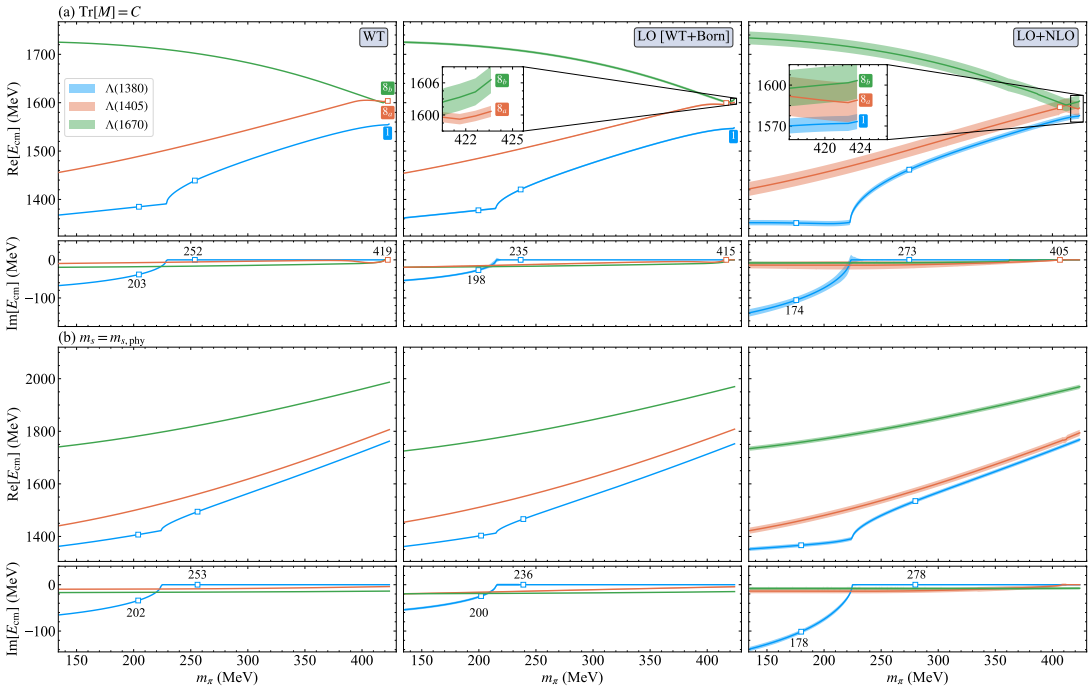

Figure 3: Trajectories of the three poles up to NLO for the $\Lambda(1405)$ and $\Lambda(1670)$ along the curve $\mathrm{Tr}[M] = C$ (a) and the curve $m_s = m_{s,\mathrm{phy}}$ (b). The uncertainties of trajectories up to NLO originate from the statistical errors and the lattice spacing error.

Acknowledgement

We are grateful to J. A. Oller, P. C. Bruns, A. Cieplý, J. R. Pelaez, S. Cruz-Alzaga, and F. Gil-Dominguez for useful discussions. We acknowedge to the BaSc Collaboration and J. Bulava, and the RQCD Collaboration for making the data available to us. R. M. acknowledges support from the ESGENT program with Ref. ESGENT/018/2024 and the PROMETEU program with Ref. CIPROM/2023/59, of the Generalitat Valenciana, and also from the Spanish Ministerio de Economia y Competitividad and European Union (NextGenerationEU/PRTR) by the grant with Ref. CNS2022-13614. L. S. G. acknowledges support from the National Key R&D Program of China under Grant No. 2023YFA1606703 and the Natural Science Foundation of China under the Grant No. 12435007.

References

[1] R.H. Dalitz and S.F. Tuan, *A possible resonant state in pion-hyperon scattering*, *Phys. Rev. Lett.* **2** (1959) 425.

[2] R.H. Dalitz and S.F. Tuan, *The phenomenological description of -K -nucleon reaction processes*, *Annals Phys.* **10** (1960) 307.

[3] E. Oset and A. Ramos, *Nonperturbative chiral approach to s wave anti-K N interactions*, *Nucl. Phys. A* **635** (1998) 99.

[4] J.A. Oller and U.G. Meissner, *Chiral dynamics in the presence of bound states: Kaon nucleon interactions revisited*, *Phys. Lett. B* **500** (2001) 263.

[5] D. Jido, J.A. Oller, E. Oset, A. Ramos and U.G. Meissner, *Chiral dynamics of the two Lambda(1405) states*, *Nucl. Phys. A* **725** (2003) 181.

[6] B. Borasoy, R. Nissler and W. Weise, *Chiral dynamics of kaon-nucleon interactions, revisited*, *Eur. Phys. J. A* **25** (2005) 79.

[7] T. Hyodo and W. Weise, *Effective anti-K N interaction based on chiral SU(3) dynamics*, *Phys. Rev. C* **77** (2008) 035204.

[8] M. Mai, *Review of the* $\Lambda(1405)$ *A curious case of a strangeness resonance*, *Eur. Phys. J. ST* **230** (2021) 1593.

[9] U.-G. Meißner, *Two-pole structures in QCD: Facts, not fantasy!*, *Symmetry* **12** (2020) 981.

[10] P.A. Zyla, R.M. Barnett, J. Beringer, O. Dahl, D.A. Dwyer, D.E. Groom et al., *Review of particle physics*, *Progress of Theoretical and Experimental Physics* **2020** (2020) 083C01.

[11] A. Feijoo, V. Magas and A. Ramos, $S{=}{-}1$ *meson-baryon interaction and the role of isospin filtering processes*, *Phys. Rev. C* **99** (2019) 035211.

[12] D. Sadasivan, M. Mai and M. Döring, *S- and p-wave structure of* $S = -1$ *meson-baryon scattering in the resonance region*, *Phys. Lett. B* **789** (2019) 329.

[13] M. Mai and U.-G. Meißner, *Constraints on the chiral unitary* $\bar{K}N$ *amplitude from* $\pi\Sigma K^+$ *photoproduction data*, *Eur. Phys. J. A* **51** (2015) 30.

[14] A. Cieplý, M. Mai, U.-G. Meißner and J. Smejkal, *On the pole content of coupled channels chiral approaches used for the* $\bar{K}N$ *system*, *Nucl. Phys. A* **954** (2016) 17.

[15] J.-X. Lu, L.-S. Geng, M. Doering and M. Mai, *Cross-Channel Constraints on Resonant Antikaon-Nucleon Scattering*, *Phys. Rev. Lett.* **130** (2023) 071902.

[16] Z.-W. Liu, J.M.M. Hall, D.B. Leinweber, A.W. Thomas and J.-J. Wu, *Structure of the* $\boldsymbol{\Lambda(1405)}$ *from Hamiltonian effective field theory*, *Phys. Rev. D* **95** (2017) 014506.

[17] P. Gubler, T.T. Takahashi and M. Oka, *Flavor structure of* Λ *baryons from lattice QCD: From strange to charm quarks*, *Phys. Rev. D* **94** (2016) 114518.

[18] J.M.M. Hall, W. Kamleh, D.B. Leinweber, B.J. Menadue, B.J. Owen, A.W. Thomas et al., *Lattice QCD Evidence that the* $\Lambda(1405)$ *Resonance is an Antikaon-Nucleon Molecule*, *Phys. Rev. Lett.* **114** (2015) 132002.

[19] S. Meinel and G. Rendon, *Charm-baryon semileptonic decays and the strange* Λ^* *resonances: New insights from lattice QCD*, *Phys. Rev. D* **105** (2022) L051505.

[20] P.C. Bruns and A. Cieplý, *SU(3) flavor symmetry considerations for the* $K^{-}N$ *coupled channels system*, *Nucl. Phys. A* **1019** (2022) 122378.

[21] R. Molina and M. Döring, *Pole structure of the Λ(1405) in a recent QCD simulation*, *Phys. Rev. D* **94** (2016) 056010.

[22] R. Pavao, P. Gubler, P. Fernandez-Soler, J. Nieves, M. Oka and T.T. Takahashi, *The negative-parity spin-1/2 Λ baryon spectrum from lattice QCD and effective theory*, *Phys. Lett. B* **820** (2021) 136473.

[23] F.-K. Guo, Y. Kamiya, M. Mai and U.-G. Meißner, *New insights into the nature of the Λ(1380) and Λ(1405) resonances away from the SU(3) limit*, *Phys. Lett. B* **846** (2023) 138264.

[24] J.-M. Xie, J.-X. Lu, L.-S. Geng and B.-S. Zou, *Two-pole structures as a universal phenomenon dictated by coupled-channel chiral dynamics*, *Phys. Rev. D* **108** (2023) L111502.

[25] X.-L. Ren, *Light-quark mass dependence of the Λ(1405) resonance*, *Physics Letters B* **855** (2024) 138802.

[26] Baryon Scattering (BaSc) Collaboration collaboration, *Lattice qcd study of* $\pi\Sigma - \overline{K}n$ *scattering and the* $\Lambda(1405)$ *resonance*, *Phys. Rev. D* **109** (2024) 014511.

[27] Baryon Scattering (BaSc) Collaboration collaboration, *Two-pole nature of the* $\Lambda(1405)$ *resonance from lattice qcd*, *Phys. Rev. Lett.* **132** (2024) 051901.

[28] G.S. Bali, S. Collins, P. Georg, D. Jenkins, P. Korcyl, A. Schäfer et al., *Scale setting and the light baryon spectrum in* $n_f = 2 + 1$ *qcd with wilson fermions*, *Journal of High Energy Physics* **2023** (2023) 35.

[29] Z. Zhuang, R. Molina, J.-X. Lu and L.-S. Geng, *Pole trajectories of the* $\Lambda(1405)$ *helps establish its dynamical nature*, 2405.07686.

[30] A. Feijoo, V.K. Magas and A. Ramos, *The* $\bar{K}N \to K\Xi$ *reaction in coupled channel chiral models up to next-to-leading order*, *Phys. Rev. C* **92** (2015) 015206.

[31] K.P. Khemchandani, A. Martínez Torres and J.A. Oller, *Hyperon resonances coupled to pseudoscalar- and vector-baryon channels*, *Phys. Rev. C* **100** (2019) 015208.

[32] R. Molina and J. Ruiz de Elvira, *Light- and strange-quark mass dependence of the ρ(770) meson revisited*, *Journal of High Energy Physics* **11** (2020) 017.

[33] J.A. Oller, *Coupled-channel approach in hadron–hadron scattering*, *Prog. Part. Nucl. Phys.* **110** (2020) 103728.

[34] X.L. Ren, L.S. Geng, J. Martin Camalich, J. Meng and H. Toki, *Octet baryon masses in next-to-next-to-next-to-leading order covariant baryon chiral perturbation theory*, *Journal of High Energy Physics* **12** (2012) 073.

[35] Y.-B. He, X.-H. Liu, L.-S. Geng, F.-K. Guo and J.-J. Xie, *Identifying the two-pole structure of the* $\Lambda(1405)$ *using an SU(3) flavor filter*, .